Stomatin-deficient cryohydrocytosis results from mutations in *SLC2A1*: a novel form of GLUT1 deficiency syndrome

Joanna F. Flatt,[1] Hélène Guizouarn,[2] Nicholas M. Burton,[1,3] Franck Borgese,[2] Richard J. Tomlinson,[4] Robert J. Forsyth,[5] Stephen A. Baldwin,[6] Bari E. Levinson,[7] Philippe Quittet,[8] Patricia Aguilar-Martinez,[8] Jean Delaunay,[9] Gordon W. Stewart,[10] and Lesley J. Bruce[1]

[1]Bristol Institute for Transfusion Sciences, NHS Blood and Transplant, Bristol, United Kingdom; [2]Institut de Biologie du Développement et Cancer Unité Mixte de Recherche 6543, Université de Nice–Centre National de La Recherche Scientifique, Nice, France; [3]Department of Biochemistry, University of Bristol, Bristol, United Kingdom; [4]Honeylands Specialist Children's Centre, Royal Devon and Exeter, United Kingdom; [5]Institute of Neuroscience, Newcastle University, Newcastle, United Kingdom; [6]Astbury Centre for Structural Molecular Biology, Institute of Membrane and Systems Biology, University of Leeds, Leeds, United Kingdom; [7]Department of Medicine, San Rafael Medical Center, San Rafael, CA; [8]Laboratoire Central d'Hematologie et Hôpital Saint-Eloi, Montpellier, France; [9]Inserm U 779, Faculté de Médecine Paris-Sud, Université Paris-Sud, Le Kremlin-Bicêtre, France; and [10]Department of Medicine, University College London, London, United Kingdom

The hereditary stomatocytoses are a series of dominantly inherited hemolytic anemias in which the permeability of the erythrocyte membrane to monovalent cations is pathologically increased. The causative mutations for some forms of hereditary stomatocytosis have been found in the transporter protein genes, *RHAG* and *SLC4A1*. Glucose transporter 1 (glut1) deficiency syndromes (glut1DSs) result from mutations in *SLC2A1*, encoding glut1. Glut1 is the main glucose transporter in the mammalian blood-brain barrier, and glut1DSs are manifested by an array of neurologic symptoms. We have previously reported 2 cases of stomatin-deficient cryohydrocytosis (sdCHC), a rare form of stomatocytosis associated with a cold-induced cation leak, hemolytic anemia, and hepatosplenomegaly but also with cataracts, seizures, mental retardation, and movement disorder. We now show that sdCHC is associated with mutations in *SLC2A1* that cause both loss of glucose transport and a cation leak, as shown by expression studies in *Xenopus* oocytes. On the basis of a 3-dimensional model of glut1, we propose potential mechanisms underlying the phenotypes of the 2 mutations found. We investigated the loss of stomatin during erythropoiesis and find this occurs during reticulocyte maturation and involves endocytosis. The molecular basis of the glut1DS, paroxysmal exercise-induced dyskinesia, and sdCHC phenotypes are compared and discussed. (*Blood*. 2011;118(19): 5267-5277)

Introduction

The hereditary stomatocytoses (HSts) comprise a group of hemolytic anemias in which there is a deleterious increase in the diffusional permeability of the erythrocyte membrane to monovalent cations, which destabilizes the osmotic balance (and therefore the volume control) of the cell. This "leak" is easily measured as the residual permeability of the erythrocyte membrane to potassium ions when the Na^+K^+ATPase and $Na^+K^+2Cl^-$ cotransporter are inhibited with ouabain and bumetanide.[1] We have previously shown that most cases of cryohydrocytosis (CHC), in which the monovalent cation leak is increased at low temperature, results from amino acid substitutions in the membrane domain of band 3 (anion exchanger 1, *SLC4A1*).[2] More recently we have shown that overhydrated hereditary stomatocytosis (OHSt), characterized by a massive cation leak at 37°C and loss of stomatin, results from amino acid substitutions in the Rh-associated glycoprotein (RhAG).[3] Band 3 and RhAG associate in the erythrocyte membrane to form a macrocomplex of proteins and may have complementary functions; band 3 is important for CO_2 transport, exchanging HCO_3^- ions for Cl^- ions, and RhAG is a putative gas channel protein.[4]

Here, we describe an extremely rare form of HSt known as stomatin-deficient CHC (sdCHC). The erythrocyte phenotype falls between CHC and OHSt. The erythrocytes have a large cation leak at low temperatures and are in this respect similar to CHC, but they also lack stomatin as in OHSt cells.[5,6] Only 2 cases have been reported, and in each case the condition is associated with a neurologic disorder and cataracts.[5] We have previously shown that sdCHC is not associated with mutations in either *SLC4A1* or *RHAG*.[7] We were prompted to investigate the glucose transporter 1 gene (*SLC2A1*) after 2 recent reports. The first showed that association of stomatin with the erythrocyte glucose transporter (glut1) switches glut1 from a glucose transporter to an L-dehydroascorbic acid transporter.[8] The second study showed that a patient with paroxysmal exertion-induced dyskinesia and a mutation in *SLC2A1* also had cation leaky erythrocytes, although in this case the erythrocytes were echinocytic rather than stomatocytic.[9]

Paroxysmal exertion-induced dyskinesia (PED) is a mild form of the ever-increasing group of glut1 deficiency syndrome (glut1DS) diseases.[10] In severe forms, there occur motor and mental developmental delay, seizures with infantile onset, and movement disorder.[10] The condition results from impaired glucose transport across the blood-brain barrier. Some symptoms of glut1DS can be ameliorated by a ketogenic diet that provides an alternative fuel for the brain.[11] Our patients both experienced seizures, developmental delay, and movement disorders, a phenotype that was strikingly

Submitted December 30, 2010; accepted July 7, 2011. Prepublished online as *Blood* First Edition paper, July 26, 2011; DOI 10.1182/blood-2010-12-326645.

The online version of this article contains a data supplement.

The publication costs of this article were defrayed in part by page charge payment. Therefore, and solely to indicate this fact, this article is hereby marked "advertisement" in accordance with 18 USC section 1734.

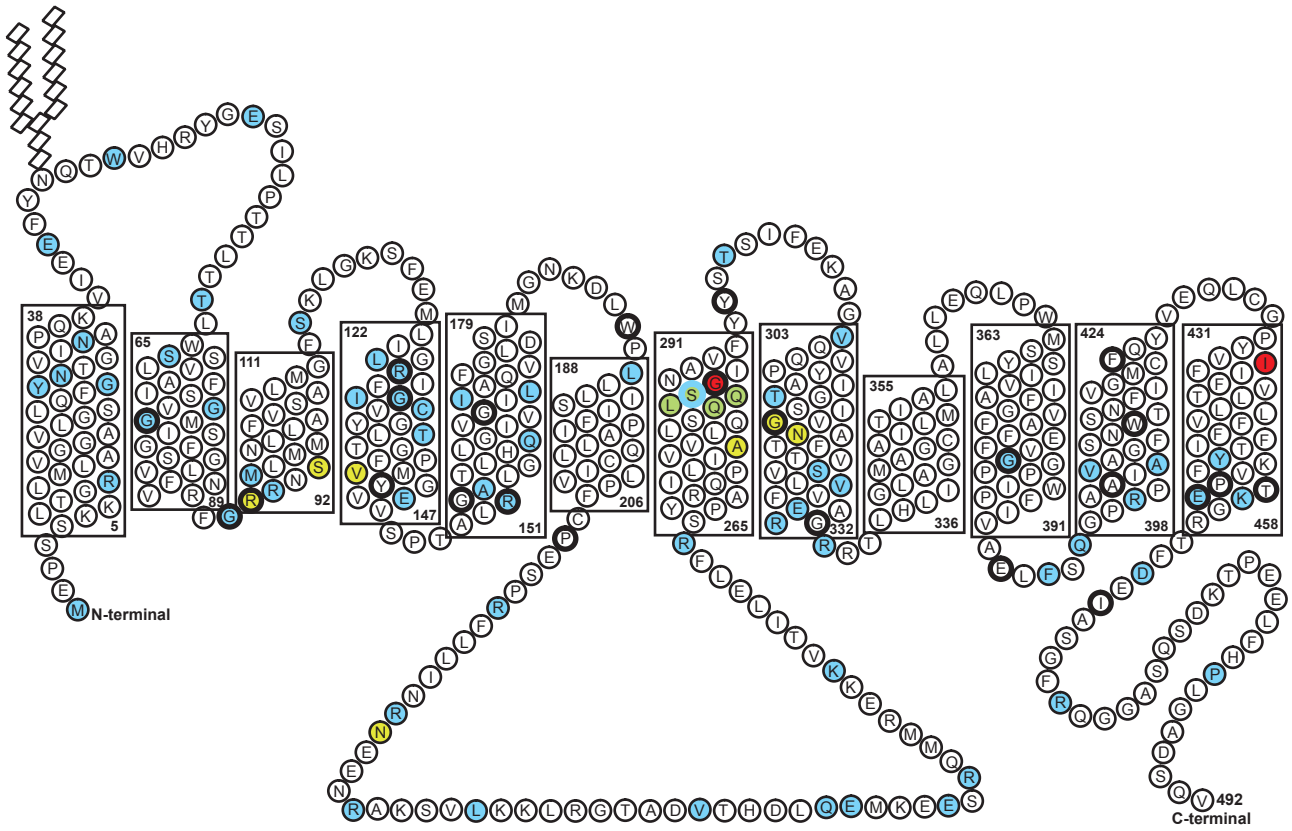

Figure 1. Schematic diagram of glut1. A schematic diagram of glut1 is shown, the membrane spans are based on the model shown in Figure 2A. Mutations (reading frame shifts, sites of insertions or substitutions) associated with glut1DS are highlighted in blue.[12,26-29,31] Glut1DS is also associated with splice site mutations and deletions (not shown). Mutations associated with PED are highlighted in light green.[30] Deletion of "QQLS" associated with PED and echinocytic anemia is highlighted in dark green.[9] Mutations associated with sdCHC are highlighted in red. The 24 amino acids with a bold outline are totally conserved residues across all glucose transporter isoforms and all species (supplemental Figures 1-2, available on the *Blood* Web site; see the Supplemental Materials link at the top of the online article).

similar to severe glut1DS. However, the phenotype of our 2 patients was distinct from typical glut1DS or the previously reported PED with a cation leak.[9] Erythrocytes from our patients lacked stomatin and were stomatocytic, and both patients had cataracts. Together, our results describe a novel glut1DS phenotype.

In these patients we have found 2 novel mutations in the *SLC2A1* gene: a GGC to GAC substitution in codon 286, resulting in the substitution of a glycine residue with an aspartic acid residue at position 286 (Gly286Asp) and the deletion of 3 nucleotides (ATC), resulting in the deletion of amino acid Ile435 or Ile436. We have expressed the mutant glut1 proteins in *Xenopus* oocytes and have shown that both mutant proteins leak cations, whereas neither transports glucose. We have modeled the effect of these mutations on glut1. With the use of confocal microscopy we have investigated the loss of stomatin during erythropoiesis in sdCHC and OHSt and find that this occurs predominantly during reticulocyte maturation and involves endocytosis.

Methods

Patients

Patients with sdCHC. Both patients have been described previously.[5,6] Patient sdCHC(A) was reported as patient D-II-2, and patient sdCHC(B) as patient E-II-1 in Fricke et al.[5] Both patients have sdCHC (OMIM 608885; http://www.ncbi.nlm.nih.gov) with leaky erythrocytes (Na^+ and K^+ transport rates increased by ~ 10-fold at 4°C), resulting in moderate hemolytic anemia with periodic hemolytic crises.[5] Hypoglycorrhachia (low cerebrospinal fluid glucose concentration) has not been tested for in these patients.

Patients with OHSt. Patient OHSt(A) was described previously.[3] Patient OHSt(B) has the same phenotype and mutation in *RHAG* (Phe65Ser) as patient OHSt(A) (G.W.S. and L.J.B., unpublished results, May 25, 2011).

Patients with Glut1DS. Both patients had classic glut1DS (OMIM 606777; http://www.ncbi.nlm.nih.gov) with hypoglycorrhachia. Patients Glut1DS(A) and Glut1DS(B) were reported as patients 26 and 18 in Leen et al.[12] Glut1DS(A) presented early with seizures, myoclonic jerks, and developmental delay. Since diagnosis at 6 years his condition has been reasonably well controlled by a ketogenic diet and ethosuximide, and he is now in special education for moderate learning difficulties. Glut1DS(B) presented with abnormal eye movements at 6 months, followed shortly by onset of seizures and global development delay. He later developed microcephaly and 4-limb spasticity with severe learning difficulties.

All samples were sent by the referring clinicians for diagnostic analysis with the informed consent of the patients or their families in accordance with the Declaration of Helsinki. This work was approved by the National Research Review Committee.

DNA sequencing analysis

Genomic DNA was isolated from blood samples. The coding regions of exons 1 to 10 of human *SLC2A1* were amplified by PCR, using exon specific primers, and the DNA was sequenced as described previously.[2] DNA sequencing was used to analyze exons 6 and 10 of *SLC2A1* from all available family members and 35 unrelated controls.

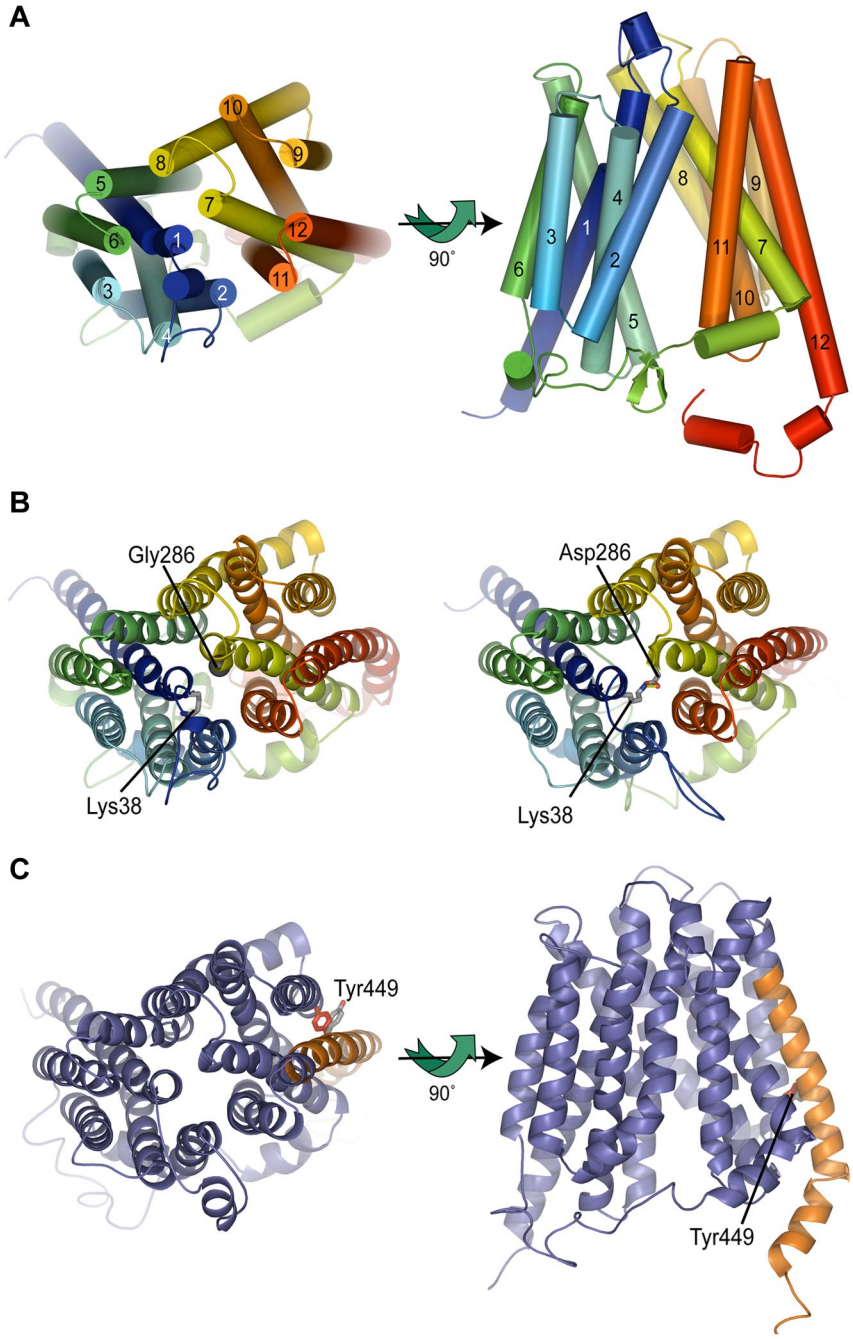

Figure 2. Homology model of glut1. (A) Structural model of wild-type glut1. Cartoon representation of glut1 model colored from blue at the N-terminus to red at the C-terminus with transmembrane helices numbered 1-12. Left panel shows the view from outside the cell; right panel shows view from within the membrane. (B) Structural model of Gly286Asp mutation. Wild-type (left) and Gly286Asp (right) homology models are displayed as Cα ribbon colored from blue at the N-terminus to red at the C-terminus. The Cα atom of Gly286 is shown as a gray sphere and side chains of Lys38 and Asp286 are displayed as sticks colored by atom type. The putative novel salt bridge between Lys38 and Asp286 is shown as a dashed yellow line. (C) Structural model of ΔIle435 mutation. Homology model of ΔIle435 glut1 is displayed as Cα ribbon. Left panel shows the view from outside the cell; right panel shows view from within the membrane. Region of the protein between Ile435 and the C-terminus is colored orange. The side chain of Tyr449 (numbered as in the wild-type protein) is shown as sticks in 2 conformations. The high-energy conformation observed in the final, refined model is shown in gray; for illustrative purposes the closest energetically favorable side chain conformation is shown in red. Adoption of this conformation would cause extensive steric clashes with the residues of transmembrane helix 9.

Erythrocyte membrane protein analysis

Preparation of erythrocyte membranes, SDS-PAGE, and Western blotting analysis of membrane proteins were performed as previously described.[4] Treatment with peptide N-glycosidase F was as described.[13] Only the sdCHC(A) sample was available for study and was typed as Rh-type "rr." Because the quantity of a number of erythrocyte proteins alters with Rh phenotype, Rh rr controls were used. Protein concentration was estimated with the Bradford assay, and equal amounts (typically 5 or 10 μg) of ghosts were loaded per track of each gel. The rabbit polyclonal antibodies to glut1 (raised against the C-terminal sequence of human glut1 [residues 477-492][14]) and stomatin, and the mouse monoclonal antibodies BRIC5 (anti-CD58) and BRIC221 (anti-Lutheran blood group glycoprotein) were used as previously described.[3,4] Western blot analyses were analyzed by semiquantitative scanning densitometry with the use of the Kodak MI Version 4.0 software (Carestream Health Inc).

Table 1. MOLPROBITY analysis of glut1 homology models

	WT	Gly286Asp	ΔIle435	1SUK
Clashscore* (percentile†)	16.58 (49th)	17.65 (44th)	15.54 (55th)	75.37 (0)
Poor rotamers, %	2.03	1.52	2.54	5.58
Ramachandran outliers, %	0.00	0.00	0.00	1.84
Ramachandran favored, %	95.93	96.36	97.00	88.98
Cβ deviations > 0.25Å	20	21	17	27
MolProbity score‡ (percentile§)	2.23 (55th)	2.13 (64th)	2.18 (60th)	3.49 (2nd)
Residues with bad bonds, %	0.00	0.00	0.00	1.42
Residues with bad angles, %	0.21	0.43	0.21	3.25

Included are details of the MOLPROBITY analysis of our glut1 homology models (WT, wild-type glut1; Gly286Asp glut1; ΔrIle435 glut1) and of a previously published glut1 model (PDB ID 1SUK[23]). 1SUK is consistent with practically all biochemical and mutagenesis data but contains significant deviations from ideal geometry when analyzed by state-of-the-art validation software. MOLPROBITY[24] ranks 1SUK in the second percentile of crystallographic structures determined at approximately 2-Å resolution (whereby the 100th percentile is the best). In contrast, our refined model of wild-type glut1 is ranked in the 55th percentile.

*Clashscore is the number of serious steric overlaps (> 0.4 Å) per 1000 atoms.

†One-hundredth percentile is the best among structures of comparable resolution; 0 percentile is the worst (N = 715; 2.00 Å ± 0.25 Å).

‡MolProbity score is defined as 0.425 74 × log(1+clashscore) + 0.329 96 × log[(1 + max(0pctRotOut-1)] + 0.249 79 × log[1 + max(0,100-pctRamaFavored-2)] + 0.5.

§One-hundredth percentile is the best among structures of comparable resolution; 0 percentile is the worst (N = 12 522; 2.00 Å ± 0.25 Å).

Culture of mononuclear cells

Human mononuclear cells were isolated from buffy coats and cultured using the method of Leberbauer et al,[15] with modifications,[16] using serum-free StemSpan Expansion Medium (StemCell Technologies) supplemented with SCF (100 ng/mL; R&D Systems), insulin-like growth factor 1 (40 ng/mL; R&D Systems), IL-3 (1 ng/mL; R&D Systems), erythropoietin (3 U/mL; Roche), dexamethasone (1mM; Sigma-Aldrich) and low-density lipoprotein (1 μL/mL; Calbiochem). Cells were seeded at 10×10^6/mL on day 0 (phase 1) and were reseeded, then maintained at a concentration of 1×10^6/mL from day 5 onward (phase 2) in vented T25 Falcon flasks (BD Biosciences) in 5% CO_2 at 37°C. Cell cultures were differentiated (phase 3) with the use of StemSpan Expansion Medium supplemented with holotransferrin (1 mg/mL; R&D Systems) and AB serum (3% vol/vol), erythropoietin (10 U/mL), insulin (10 ng/mL), and 3,5,3′-triiodo-L-thyronine (1μM) from Sigma-Aldrich.

Confocal microscopy

Early stage cells were seeded on 0.01% (wt/vol) poly-L-lysine (Sigma-Aldrich) coated coverslips (0.5×10^6 cells per coverslip) and incubated 1 hour at 37°C in 5% CO_2. Cells were fixed with 3% formaldehyde (TAAB) for 20 minutes and permeabilized with 0.05% (wt/vol) digitonin (Sigma-Aldrich) for 5 minutes. Antibody application and imaging were done as described.[17] Late stage cells/reticulocytes were seeded as described earlier but fixed in 1% formaldehyde and permeabilized in 0.05% (wt/vol) saponin (Sigma-Aldrich) with subsequent washes and incubations, including 0.005% (wt/vol) saponin. Mature erythrocytes were seeded as mentioned earlier, incubated 20 minutes at room temperature, then fixed in 1% formaldehyde plus 0.0075% glutaraldehyde and permeabilized in 0.1% (wt/vol) Triton X-100 (Sigma-Aldrich). Primary antibodies used were rabbit polyclonal anti-glut1,[14] mouse monoclonal anti-stomatin (GARP50[18]), and rabbit polyclonal anti-transferrin receptor (Abcam). Goat anti–mouse Alexa Fluor 488 or goat anti–rabbit Alexa Fluor 546 secondary antibodies were used. Samples were imaged at 19°C with the use of ×40 oil-immersion lenses on a Leica DMI6000 B inverted microscope with phase contrast connected to a Leica TCS-SP5 confocal laser scanning microscope (Leica). Images were obtained using Leica LAS software (LAS AF 1.6.3 build 1163) and subsequently processed using Adobe Photoshop.

Preparation of mutant constructs and expression in *Xenopus laevis* oocytes

The cDNA clone, pBS/KS-glut1, was prepared by inserting a *Bam*HI fragment containing the entire coding region of glut1 from the original pSGT-glut1 clone[19] into the *Bam*HI site of pBluescript II KS(+). We found that this original clone coded for phenylalanine at position 152. Amino acid 152 is now known to be a leucine residue (Human Genome project; http://www.ncbi.nlm.nih.gov/genome/guide/human/). Therefore, we first corrected the pBS/KS-glut1 clone by substituting Phe152 with Leu152 with the use of the Quikchange II mutagenesis kit (Strategene) with the use of pBS/KS-glut1 as a template and the primers Phe152Leu sense, tcacccacagc-ccttcgtggggccc, and Phe152Leu antisense, gggccccacgaagggctgtgggtga.

The amino acid substitution Gly286 to Asp286 and the deletion of amino acid Ile435 or Ile436 (one "ATC" was deleted from the sequence) were made with the Quikchange II mutagenesis kit (Strategene) with the use of $pBS/KS\text{-}glut1_{corrected}$ as a template and the following primers: Gly286Asp sense, cccagcagctgtctgacat-caacgctgtctt, and Gly286Asp antisense, aagacagcgttgatgtcagacagctgctggg; ΔIle435 sense, actgtgtggtccctacgtcttcatcttcactgtg, and ΔIle435 antisense, cacagtgaagatgaagacgtagggaccacacagt.

The sequences of the final constructs were confirmed by automated sequencing (ABI PRISM 3100 Genetic Analyzer Automatic Sequencer; Applied Biosystems). The methods used for the preparation of cRNA, expression in oocytes, and measurement of Na^+ and K^+ content by flame photometry have been described.[2] The method used for the measurement of oocyte Li^+ influx has been described.[3,20]

Immunoblotting of expressed protein in oocytes

Oocyte membranes were prepared as described previously,[21] and separated on 10% SDS-PAGE as described.[3] Western blots were probed with the rabbit polyclonal anti-glut1 antibody[14] (1:40 000).

Deoxy-D-glucose uptake measurements in oocytes

Oocytes dedicated to glucose uptake measurements and membrane cryosectioning were injected with 20 ng of cRNA and incubated for 48-72 hours at 18°C in OR3 medium with the following composition: $CaCl_2$, 0.74mM; $MgCl_2$, 0.58mM; $MgSO_4$, 0.48mM; KCl, 3.1mM; KH_2PO_4, 0.26mM; NaCl, 81mM; Na_2HPO_4, 0.79mM; D+ galactose, 2.9mM; sodium pyruvate, 2.9mM; penicillin, 100 U/mL; and streptomycin, 100 μg/mL. The oocytes were then transferred to Modified Barth Solution (MBS) with the following: NaCl, 88mM; KCl, 1.0mM; $NaHCO_3$, 2.4mM; HEPES, pH 7.6, 10mM; $CaCl_2$, 0.41mM; $Ca(NO_3)_2$, 0.33mM; $MgSO_4$, 0.82mM; sodium pyruvate, 2.5mM; penicillin, 20 IU/mL; and streptomycin, 0.02 mg/mL. Transfer was > 18 hours before the glucose uptake experiment to allow equilibration to the medium change. Oocytes (5 per condition) were incubated in MBS or MBS containing phloretin (100μM) and cytochalasin B (50μM) for 20 minutes at room temperature and then incubated for 20 minutes (within the linear phase of glucose influx) with gentle agitation in 2-[^{3}H(G)]-deoxy-D-glucose solution (25μM 2-deoxy-D-glucose, 0.5 μCi/mL [0.0185 MBq/mL] in MBS), then washed 3 times with stop solution (100μM phloretin in PBS, ice cold). Oocytes were solubilized in 1% SDS solution, and radioactivity was measured with a scintillation counter.

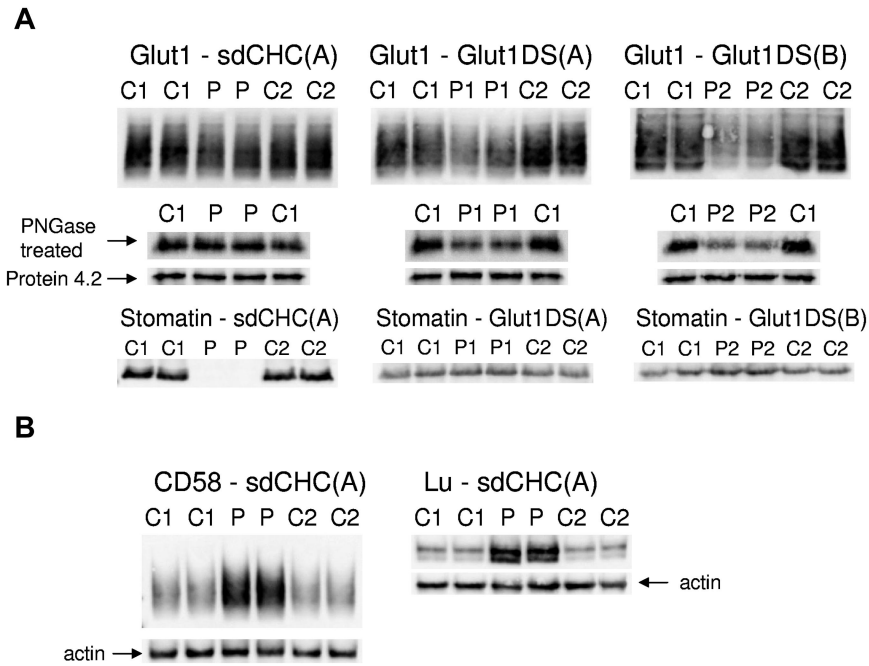

Figure 3. Erythrocyte membrane protein analysis. Erythrocyte membranes were separated on 10% Laemmli gels and immunoblotted with the use of antibodies as shown. Loading: C1, C2, controls 1 and 2. P indicates proband [sdCHC(A)] except where labeled as glut1DS patient A or B. (A) The glut1 protein is heavily glycosylated (seen as a broad 50- to 100-kDa band). Scanning densitometry analysis of the deglycosylated glut1 band (labeled PNGase treated) showed normal amounts of glut1 in the patients with sdCHC and reduced amounts of glut1 (by ~ 40%) in the patients with glut1DS. A protein 4.2 loading control is shown beneath each blot. The reduction in stomatin has been shown previously and is characteristic of sdCHC. Stomatin was present in normal amounts in the patients with glut1DS. (B) Both CD58 and Lutheran protein were increased in the sdCHC sample. An actin loading control is shown beneath each blot.

Cryosectioning and immunohistochemical staining of oocytes

Glut1 expression at the plasma membrane of oocytes was confirmed by immunofluorescence microscopy as described previously.[22] Permeabilization and staining of oocytes were performed as described previously[22] but with the use of an anti-glut1 rabbit polyclonal antibody[14] (1:5000 in 4% BSA) and goat anti–rabbit Alexa Fluor 546–conjugated secondary antibody (1:500).

Structural modeling of the mutant glut1 proteins

The crystallographically determined structure of the *Escherichia coli* glycerol-3-phosphate transporter (PDB ID 1pw4[23]) was used as a template to build homology models of the wild-type and mutant glut1 proteins with the use of the MODELLER Version 9v6 software[24] and the National Center for Biotechnology Information reference sequence NP_006507.2 that contains a leucine at position 152. Twenty models were generated for each of the wild-type and mutant glut1 proteins. The large unaligned loop regions (residues Glu43-Thr62, Pro208-Met252, and Gln469-Val492) were further optimized with the MODELLER "dope_loopmodel" routine. One hundred models were generated for each loop and scored with the DOPE function.[24] Ten models for each isoform with the best overall DOPE scores were superposed and visually inspected. The 3 models (wild-type, Gly286Asp, and ΔIle435) with the best overall DOPE scores were selected for further analysis. The quality of each model was assessed with MOLPROBITY.[25]

Statistics

Statistical significance was calculated with the 2-tailed, unpaired Student *t* test.

Results

DNA analysis

DNA analysis of the *SLC2A1* gene in patient sdCHC(A) showed a GGC to GAC point mutation in codon 286, leading to Gly286Asp amino acid substitution. In patient sdCHC(B), we found a 3-nucleotide deletion (ATC), leading to the deletion of either Ile435 or Ile436 (YVFIIFTVLL to YVFIFTVLL; Figure 1). The Gly286Asp substitution was not found in the parents or 2 siblings of patient sdCHC(A). Relatives of patient sdCHC(B) were not available for study. Both the Gly286Asp substitution and the Ile435 deletion are presumed to be spontaneous de novo mutations. Neither mutation was found in 35 normal control DNAs. These are novel glut1 mutations and differ from those reported in other patients with glut1DS or PED (Figure 1).[9,12,26-31] The *SLC2A* family of proteins is highly similar across all 13 isoforms (supplemental Figure 1). *SLC2A1* is highly conserved across all species (supplemental Figure 2). Ile435 and Ile436 are almost completely conserved across all the species examined (supplemental Figure 2), and Gly286 is 1 of only 24 residues in the glucose transporter family that are completely conserved across all species and isoforms (supplemental Figures 1-2).

Glut1 modeling

We examined the structural basis for the cation leak and loss of glucose transport activity caused by the Gly286Asp and ΔIle435 mutations with the use of our refined glut1 models (Figure 2A). Full details of the MOLPROBITY analysis of all glut1 models are given in Table 1. Our model of wild-type glut1 predicts that Gly286 lies adjacent to the putative glucose transport pathway (Figure 2B). This is consistent with the findings of Salas-Burgos et al,[32] who predicted that Gly286 would form part of an exofacial glucose binding site. Our model of Gly286Asp glut1 predicts the potential formation of a novel salt bridge between Asp286 and Lys38, which lies on the N-terminal membrane span (TM1; Figure 2B). This salt bridge would probably reduce the conformational mobility of the protein in this key region, explaining the lack of glucose transport in this mutant. Even in the absence of salt bridge formation, the Gly286Asp mutation is probably deleterious for glucose transport. Hruz and Mueckler[33] showed that the more conservative mutation of Gly286 to cysteine reduced activity by 75%, possibly because of the proximity of Gly286 to residues Gln282 and Gln283, which have been postulated to form hydrogen bonds to glucose.

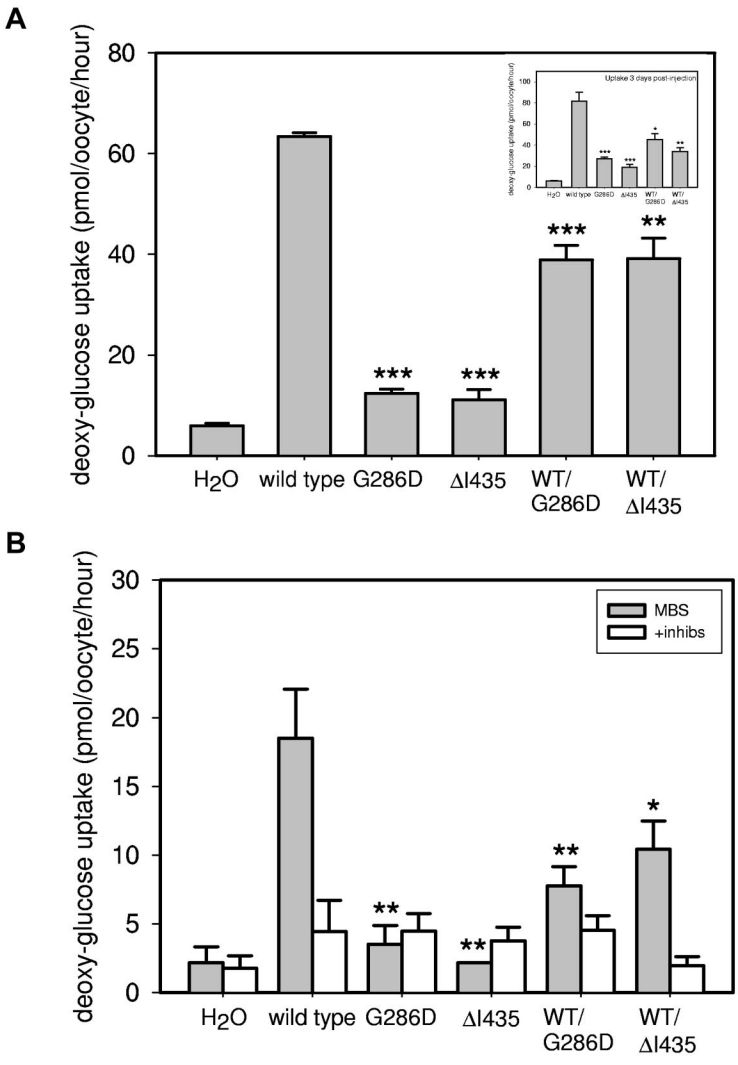

Figure 4. Glucose uptake into *Xenopus laevis* oocytes expressing wild-type or mutant glut1. Oocytes were injected with 20 ng of WT or mutant glut1 (or 10 ng of WT and 10 ng of mutant where coexpressed). Oocytes expressing WT or mutant glut1 were assayed 2 days after injection (data are means ± SEMs of 4 replicates of 5 oocytes; n = 4). $^{*}P < .05$, $^{**}P < .01$, and $^{***}P < .001$. (A) Deoxy-D-glucose uptake in *Xenopus laevis* oocytes. Inset: continuing the same experiment with oocytes assayed 3 days after injection (data are means ± SEMs of 4 replicates of 5 oocytes; n = 4). (B) Inhibition of deoxy-D-glucose uptake in *Xenopus laevis* oocytes. Oocytes were incubated in MBS or MBS containing phloretin (100μM) and cytochalasin B (50μM) for 20 minutes at room temperature before adding [^{3}H]-deoxy-D-glucose (data are means ± SEMs of 4 replicates of 5 oocytes; n = 4).

The ΔIle435 mutation removes a single amino acid from the C-terminal membrane span (TM12), which forms extensive contacts with TM7. All of the residues in TM12 are tolerant to substitution with cysteine,[34] consistent with this helix having no direct role in formation of the transport pathway. However, residues Y^{432}VFII in the N-terminal, extracellular end of TM12 are PCMBS-sensitive when mutated to cysteine,[34] suggesting that at some stage of the transport cycle these residues are exposed to extracellular solvent. Other models of glut1 suggest Y^{432}VFII may even be permanently solvent exposed.[35] The change in sequence register caused by the ΔIle435 mutation results in residues C-terminal of Ile436 on TM12 (437-458; see Figures 1 and 2C) shifting to the *i*-1 position on the α-helix, relative to their position in the wild-type protein. The homology model of ΔIle435 glut1 predicts that between residues Phe437 and Thr448 these changes could be easily accommodated with the existing protein fold. However, the side-chain of Tyr449 is too bulky to fit in the small pocket formed by the close packing of TM9 and TM12 in this region (Figure 2C). For the overall fold to be maintained, Tyr449 is forced to adopt an energetically unfavorable side-chain conformation. Therefore, the mutation may be accommodated by larger, longer-range conformational changes that would be difficult to predict accurately.

Erythrocyte membrane protein analysis

Immunoblotting analysis of sdCHC erythrocyte membranes [sdCHC(A)] confirmed the reduction of stomatin, as described previously[5,6] (Figure 3A) and showed that most other major membrane proteins, band 3, RhAG, CD47, glycophorin A, glycophorin B, protein 4.2, protein 4.1, p55, flotillin 1, CD44, CD59, DAF, AQP1, and LW, were present in normal amounts (data not shown). Two adhesion proteins, the Lutheran blood group glycoprotein (basal cell adhesion molecule, CD239) and the lymphocyte function-associated protein 3 (CD58) were increased in sdCHC(A) membranes (Figure 3B). This increase has been noted before in other hemolytic anemias, but the cause is not known[4] (L.J.B., unpublished results, April 2010). Immunoblotting analysis showed the glut1 protein from sdCHC(A) erythrocytes was expressed at normal levels compared with control glut1 (Figure 3A). Semiquantitative scanning densitometry analysis of the deglycosylated bands showed that glut1 protein in sdCHC(A) was 101% that of control. By contrast, immunoblotting of erythrocyte membranes from 2 patients with glut1DS showed that they have reduced glut1 levels but normal stomatin levels (Figure 3A). Semiquantitative scanning densitometry analysis of the deglycosylated bands showed that glut1 protein in both glut1DS(A) and glut1DS(B) was ~ 63% that of control. These results suggest that, although the glut1DS

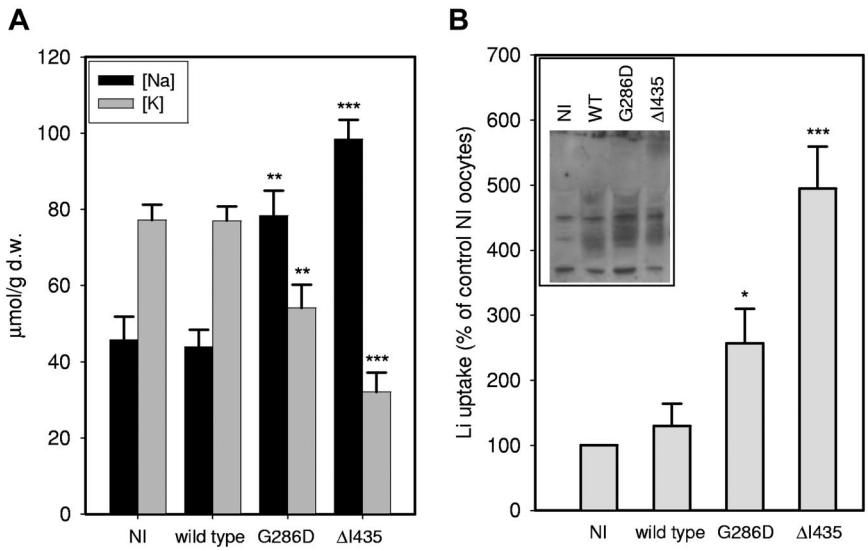

Figure 5. Cation leak in *Xenopus laevis* oocytes expressing wild-type or mutant glut1. (A) Intracellular sodium and potassium ion concentrations were measured by flame photometry on washed, extracted oocytes (3 replicates of 5 oocytes per condition) after 72 hours of incubation at 19°C in MBS containing ouabain (0.5mM) and bumetanide (5μM). Data, expressed in μmol/g of dry weight, are the mean values ± SEMs for 4 separate experiments; n = 12. $^{*}P < .05$, $^{**}P < .01$, and $^{***}P < .001$. (B) Li^+ influx (as a surrogate for Na^+) was measured 2 days after injection. Oocytes (7 per condition) were incubated for 2 hours at 19°C in medium in which NaCl was substituted by $LiNO_3$ in the presence of ouabain (0.5mM) and bumetanide (5μM). Li^+ content in each oocyte extract was measured by atomic absorption spectrometry with a Perkin Elmer AAS 3110. The graph shows the data from 7 repeat experiments. To normalize the data, in each individual experiment NI was taken as 100%, and the Li uptake in wild-type, glut1-G286D, and glut1-ΔI435 was expressed as a percentage of NI. The 7 values were then averaged and plotted, ± SEM; n = 7. $^{*}P < .05$, $^{**}P < .01$, and $^{***}P < .001$. Inset: Glut1 expression levels in *Xenopus laevis* oocytes were assessed by immunoblotting with the use of an antibody to the C-terminal region of glut1.

erythrocytes only express wild-type glut1, the sdCHC erythrocytes express both the wild-type and the mutant glut1 proteins.

Deoxy-D-glucose transport in oocytes

Uptake of deoxy-D-glucose was measured in *Xenopus* oocytes. Two days after cRNA injection (or 3 days after; Figure 4A inset) the water-injected oocytes showed minimal deoxy-D-glucose uptake, whereas wild-type glut1 (glut1-WT) oocytes showed a large uptake (~ 63 pmol/oocyte/hour). Oocytes expressing the glut1-Gly286Asp or glut1-ΔIle435 mutants showed minimal uptake (~ 12 pmol/oocyte/hour), and oocytes coexpressing mutant and glut1-WT showed ~ 50% of glut1-WT uptake (~ 39 pmol/oocyte/hour; Figure 4A). In a different experiment, uptake of deoxy-D-glucose was measured in *Xenopus* oocytes with and without the glucose transporter inhibitors phloretin (100μM) and cytochalasin B (50μM). In the absence of inhibitors, no significant difference was observed between the deoxy-D-glucose uptake in water-injected oocytes and in oocytes expressing the glut1-Gly286Asp or glut1-ΔIle435 mutants, suggesting that the mutant proteins do not transport glucose (Figure 4B). As before, oocytes coexpressing mutant and glut1-WT showed ~ 50% of glut1-WT uptake (Figure 4B). In the presence of inhibitors deoxy-D-glucose uptake was reduced to about the same level in all oocytes. Uptake of 3-O-methyl-D-glucose was also measured, and oocytes expressing the glut1-Gly286Asp or glut1-ΔIle435 mutants showed minimal uptake of 3-O-methyl-D-glucose (supplemental Figure 3). Immunocytochemistry of oocyte slices showed that all glut1 constructs were expressed in the oocyte membrane (supplemental Figure 4).

Cation transport in oocytes

The mutant glut1 proteins were expressed in *Xenopus* oocytes, and cation leak was measured. Normal levels of the intracellular cations Na^+ and K^+ were found in non-injected (NI) *Xenopus* oocytes and those expressing glut1-WT, whereas the levels of these cations were altered in oocytes expressing glut1-Gly286Asp or glut1-ΔIle435 (Figure 5A). Li^+ influx was minimal in oocytes and those expressing glut1-WT, whereas expression of glut1-Gly286Asp or glut1-ΔIle435 increased Li^+ influx (Figure 5B). All glut1 constructs were shown to be expressed in the oocyte (Figure 5B inset).

Confocal imaging

The expression of glut1 and stomatin were imaged in early and late erythroblasts cultured from mononuclear cells (isolated from peripheral blood) and in peripheral blood from control, sdCHC(A), and OHSt(A) samples. Stomatin and glut1 are expressed at the plasma membrane of early erythroblasts from both control and sdCHC cells (Figure 6A). Stomatin was still present and colocalized with glut1 in the plasma membrane of both control and sdCHC cells at the reticulocyte stage (Figure 6B). However, sdCHC reticulocytes also showed more internal stomatin than controls, appearing in vesicles or as an aggregate at the reticulocyte/nuclear junction (Figures 6B,7). Control peripheral blood erythrocytes showed colocalization of stomatin and glut1 at the membrane in all cells, whereas stomatin was only present in a minority of sdCHC erythrocytes, probably the reticulocytes or immature erythrocytes (Figure 6C). These results suggest that in sdCHC cells stomatin is lost late, during reticulocyte maturation. This result was unexpected because in a previous study we had shown that stomatin was lost from OHSt(A) cells during early erythropoiesis.[36] To make a direct comparison between the 2 stomatin-deficient cell types, we cultured OHSt(A) erythroblasts under the same conditions used for the sdCHC cell culture. We found that glut1 was present in the internal compartments and at the plasma membrane in the early erythroblasts from both control and OHSt(A) cells (Figure 6D). However, stomatin remained intracellular in these early OHSt(A) cells (Figure 6D). This result confirms our previous study[36] and shows that the timing and mechanism of stomatin loss differs between these OHSt(A) and sdCHC cells. It was not possible to culture these OHSt(A) erythroblasts to the reticulocyte stage; however, peripheral blood erythrocytes from this patient[3] showed some limited expression of stomatin in a few cells (Figure 6E), showing that some stomatin does manage to move to the plasma membrane in these cells. With a different culture system (see supplemental Figure 5 legend) we successfully cultured a second OHSt sample [OHSt(B)] through to the reticulocyte stage. OHSt(B) cells gave an expression profile that was somewhere between sdCHC and OHSt(A). Some OHSt(B) cells expressed stomatin in the intracellular compartments, but the cells also showed weak expression of stomatin at the plasma membrane of early

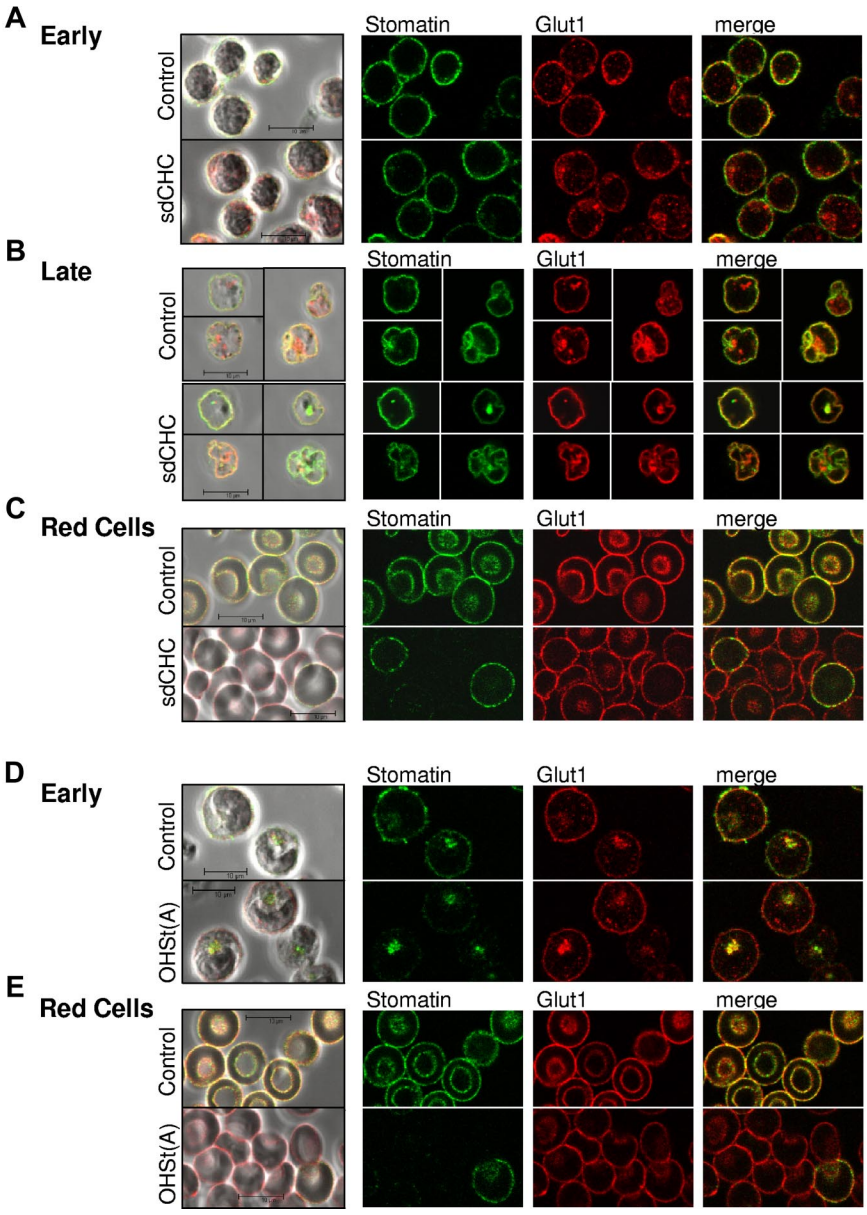

Figure 6. Confocal imaging of cultured erythroblasts. (A) Confocal imaging of cultured early stage sdCHC and control erythroblasts probed with anti-glut1 (red) and anti-stomatin (green). (B) Confocal imaging of cultured late-stage sdCHC and control reticulocytes probed with anti-glut1 (red) and anti-stomatin (green). (C) Confocal imaging of peripheral blood from sdCHC and control probed with anti-glut1 (red) and anti-stomatin (green). (D) Confocal images of cultured early-stage OHSt(A)^3 erythroblasts probed with anti-glut1 (red) and anti-stomatin (green). (E) Confocal images of peripheral blood from OHSt(A)^3 probed with anti-glut1 (red) and anti-stomatin (green).

erythroblasts and expression of stomatin in the reticulocyte membrane (supplemental data; Figure 5).

Together these results suggested that stomatin may be involved in the removal of misfolded or obsolete proteins from the maturing reticulocyte. To further characterize the internal stomatin staining in control and sdCHC reticulocytes we therefore costained with various internal markers. No colocalization was found with anti-LAMP2 (a lysosomal marker) or anti-CD63 (a late endosome marker; data not shown), but some colocalization was found, more markedly in the sdCHC reticulocytes, with anti-CD71 that binds to the transferrin receptor (an endosomal marker that is lost during reticulocyte maturation; Figure 7). Further studies are planned to clarify the role of stomatin in reticulocyte maturation.

Discussion

This study describes the mutations in 2 unrelated patients with a novel syndrome of cation-leaky stomatocytic hemolysis, cataracts, developmental neurologic delay, and seizures. We have shown that these patients with sdCHC are heterozygous for different mutations in *SLC2A1*, which codes for glut1, a glucose transporter. Many mutations in the *SLC2A1* gene have been associated with glut1DS (some of which are shown in Figure 1). Glut1DS is a condition whereby haploinsufficiency for glut1 restricts the availability of glucose in the CNS, causing hypoglycorrhachia, early-onset epilepsy resistant to anticonvulsants, slowing of head growth, developmental delay, and a complex movement disorder.[26] These mutations are normally heterozygous and often code for an unstable mRNA or protein, leading to a 50% loss of glut1 protein (as seen in Figure 3). Total loss of glut1 activity is lethal as shown in the mouse model for glut1DS.[37] Hemolytic anemia has not previously been reported in these patients with classic glut1DS, suggesting that haploinsufficiency of glut1 is not critical in erythrocytes. Loss of glut1 activity in other tissues similarly may not be critical or may be compensated for by alternative glucose transporters.

Milder forms of glut1DS are probably caused by mutations in *SLC2A1* that simply reduce the rate of glucose transport. One such subtype of glut1DS is familial PED with epilepsy, whereby the

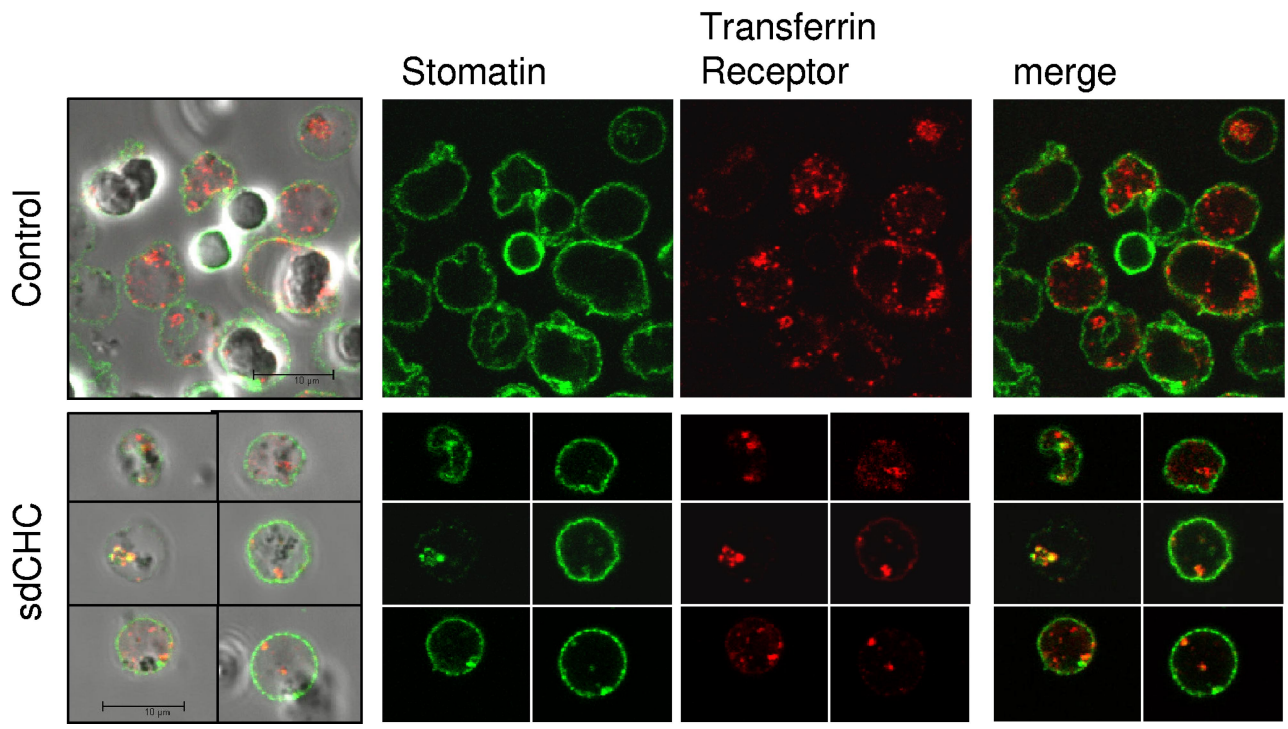

Figure 7. Colocalization of stomatin with endosomal marker CD71. Confocal imaging of cultured late-stage control and sdCHC reticulocytes probed with anti-stomatin (green) and anti-CD71 (transferrin receptor, red). The z-stack of sdCHC and control reticulocytes was examined, and the number of internal vesicles in which stomatin appeared, or TfR appeared, or in which the proteins colocalized, was noted. On average control reticulocytes contained 3 stomatin-positive vesicles per cell (n = 55 cells examined), whereas sdCHC reticulocytes contained 6 stomatin-positive vesicles per cell (n = 27 cells examined). In control cells ~ 30% of the stomatin-positive vesicles colocalized with transferrin receptor. In sdCHC cells ~ 60% of the stomatin-positive vesicles colocalized with transferrin receptor.

involuntary dystonic, choreoathetotic, and ballistic movements occur after prolonged exercise and affect only the exercised limbs (mutations shown in Figure 1).[30] It has been suggested that the severity of the phenotype of glut1DS correlates with the type of mutation.[38] To expand on this theory, we would hypothesize that the phenotype reflects both the amount of glut1 protein expressed, the activity of the glut1, and whether the expressed protein is misfolded so that it leaks cations. In Table 2 we compare what is known of the different phenotypes of glut1DS and PED with or without anemia. Our results suggest that (1) haploinsufficiency for glut1, or expression of transport defective glut1, causes neurologic symptoms but is asymptomatic in the lens or erythrocyte; (2) ex-pression of cation-leaky mutant glut1 in the erythrocyte membrane causes hemolytic anemia; and (3) expression of cation-leaky, mutant glut1 in the lens epithelium may cause cataracts (see "Cataracts").

The extent to which glut1 is expressed in erythrocytes has not always been investigated in glut1DS. We show here that in 2 cases of classic glut1DS the amount of glut1 in the erythrocyte membrane is reduced to ~ 60% of normal (Figure 3). In the previous study of PED with anemia the amount of glut1 in the erythrocyte membrane was not measured, although expression and trafficking of the 3 mutant proteins (ΔQQLS, G314S, and A275T) in *Xenopus* oocytes was normal.[9] In our case of glut1DS with hemolytic anemia [sdCHC(A)] we show that the mutant protein is expressed (Figure 3) and leaks cations (Figure 5) but displays little glucose transport activity (Figure 4).

Erythrocyte cation leak

Previous cation-leaky erythrocyte conditions have been shown to be caused by mutations in other large multispanning membrane proteins. Non–stomatin-deficient CHC results from mutations in *SLC4A1*[2,39-41] and OHSt from mutations in *RHAG*.[3] Here we show that the cation leak in sdCHC results from mutations in *SLC2A1*. Together these results show that large multispanning proteins have the capacity to leak cations if they are both misfolded and present in the plasma membrane. They may do this simply by disrupting the lipid membrane or by allowing cations to pass through the mutant transport channel.

Erythrocyte structure

The difference in erythrocyte structure between the previous study of PED with hemolytic anemia[9] and our patient with sdCHC may be because of the permeability of the erythrocytes to Ca^{2+} ions. In the study of PED with hemolytic anemia the mutant glut1 (ΔQQLS) was shown to cause a leak of Na^+, K^+, and Ca^{2+} ions when expressed in oocytes.[9] Leak of Ca^{2+} ions can activate the Gardos channel in erythrocytes, causing loss of KCl, dehydration, and echinocytosis. In the present study permeability to Ca^{2+} ions, Gardos channel activity, or phosphatidyl-serine exposure was not tested, but it was shown that the mutant glut1 proteins (Gly286Asp; ΔIle435) caused a leak of Na^+ and K^+ ions when expressed in oocytes. This leak in erythrocytes causes an increase in mean cell volume and stomatocytosis.[5]

Cataracts

A further significant difference between the patients with sdCHC and the patients with classic glut1DS is the occurrence of lens cataract. To our knowledge glut1DS and PED have not been associated with cataracts, so it is unlikely that the cataracts in our patients are caused by lack of glucose in the lens. Presumably the functionally haploid status of glut1 transport in these patients is sufficient to maintain lens metabolism. In our patients, it can be argued that the cataract may be because of Na^+ and K^+ leakage through the lens epithelium. Glut1 is expressed in the lens

Table 2. Comparing glut1 deficiency conditions

	Glut1DS	PED	PED + anemia	sdCHC + anemia
Hypoglycorrhachia	Yes	Yes	NK	NK
Seizures	Yes	Yes	Yes	Yes
Mental retardation	Yes	Mild	Mild	Yes
Growth retardation	Yes	Mild	Mild	Yes
Movement disorder	Yes	Yes	Yes	Yes
Hemolytic anemia	No	No	Yes	Yes
Hepatosplenomegaly	No	No	Yes	Yes
Stomatin-deficient	No	NK	NK	Yes
Monovalent cation leak	No	No	Yes	Yes
Ca^{2+} leak	No	No	Yes	No
RBC structure	Normal?	Normal?	Echinocytic	Stomatocytic
Cataracts	No	No	No	Yes
Cation leaky glut1 in blood/brain barrier	No	No	No	Possibly
Cation leaky glut1 in lens epithelium	No	No	No	Probably
Cation leaky glut1 in red cell membrane	No	No	Yes	Yes

NK indicates not known; and RBC, red blood cell.

epithelium, the coating around the anterior pole of the lens.[42] This epithelium has a role in the control of the water content of lens; it enables a convective flow within the interior of the lens that is thought to provide nourishment to the fiber cells of the interior, which is avascular.[43] Abnormalities in ion and water transport mechanisms have previously been suggested to be important in cataract formation.[44,45] We would hypothesize that cataracts are formed in the patients with sdCHC because the mutant (misfolded) glut1 protein is expressed in the lens epithelium where it leaks cations and undermines this convective microcirculatory system.

Stomatin loss

Stomatin, also known as band 7.2b, is a monotropic, oligomeric, lipid raft-associated protein involved in membrane organization, cholesterol-dependent regulatory processes, and possibly regulation of ion channels.[46] Stomatin is deficient in both sdCHC and OHSt, both conditions that feature extreme erythrocyte cation leaks; however, the reason for the stomatin depletion in these conditions is not known. Stomatin is known to associate with glut1,[47] decreasing its affinity for glucose[8] or targeting glut1 to lipid rafts on glucose deprivation.[48] Previously, we hypothesized that the loss of stomatin in these leaky, energy-depleted erythrocytes occurred to allow maximum glucose transport.[3]

We have studied the loss of stomatin in OHSt and sdCHC erythroblasts during erythropoiesis to make a direct comparison between the 2 cell types. We found that stomatin expression at the plasma membrane of early and late erythroblasts varied sdCHC > OHSt(B) > OHSt(A). Thus, stomatin-deficient red cells display a spectrum of expression levels during erythropoiesis, suggesting that stomatin has a complex role in these variant cells. In sdCHC and OHSt(B) reticulocytes some of the stomatin appeared intracellular, in fairly large vesicles or aggregates. Staining with various internal markers showed some colocalization of stomatin with anti-CD71 that binds to the transferrin receptor, an endosomal marker lost during reticulocyte maturation (Figure 7). Membrane stomatin expression in mature erythrocytes occurred in only a few sdCHC and OHSt cells, and these may represent reticulocytes (Figure 6C,E; supplemental Figure 5). So it is probable that stomatin is lost in the final stages of reticulocyte maturation in the circulation and involves endocytosis. The exact role of stomatin in the erythrocyte membrane is not known, but together these results suggest that stomatin may be involved in the removal of misfolded or obsolete proteins from the maturing reticulocyte. Interestingly, a recent study of low potassium dog erythrocytes (which lack both Na^+K^+ATPase and stomatin) showed that stomatin was lost, together with the Na^+K^+ATPase, at the reticulocyte maturation stage,[49] and stomatin has been shown previously to be associated with exosomes from human reticulocytes.[50]

In conclusion, we have described here a new syndrome of glut1DS with hemolytic anemia and cataracts, also known as sdCHC. Glut1DS can be alleviated by a ketogenic diet,[26] and this diet may benefit our patients with sdCHC. We have shown that our patients are not only haploinsufficient for glucose transport but also that their cells almost certainly express the mutant glut1 proteins, causing further problems. In erythrocytes the mutant glut1 is associated with a cation leak that causes stomatocytosis and hemolysis, leading to anemia and splenomegaly. In the CNS, although the primary problem is insufficient functional glut1, the cation leak may exacerbate the neurologic symptoms. In the lens epithelium the cation leak may disrupt the microcirculatory system, causing cataracts. Our data resolve the molecular cause of sdCHC and suggest a novel mechanism of cataract formation.

Acknowledgments

The authors thank P. Martin for DNA sequencing; R. Griffiths and A. Toye for confocal imaging and cell culture expertise; M. Wilson, B. Nancolas, and A. Halestrap for assistance with oocyte experiments; J. Patel for providing patient blood samples; M. Mueckler (Washington University) for the pSGT-glut1 clone; A. Weinglass for preparation of the BS/KS-glut1 clone; and the patients and their families for their cooperation.

The work was supported by the UK National Health Service R & D Directorate (J.F.F., N.M.B., and L.J.B.). G.W.S. thanks Advocacy for Neuroacanthocytosis for generous funding.

Authorship

Contribution: J.F.F. conducted DNA and protein analyses, deoxy-D-glucose transport, expression studies in *Xenopus laevis* oocytes, and confocal microscopy; H.G. and F.B. conducted cation transport and Western blots in *X laevis* oocytes; N.M.B. conducted modeling studies; R.J.T., R.J.F., B.E.L., P.Q., and P.A.-M. reexamined patients and provided samples; S.A.B. provided glut1 clone and antibody; J.D. and G.W.S. provided patient samples and prepared

the manuscript; and L.J.B. designed the research, conducted protein analysis, and prepared the manuscript.

Conflict-of-interest disclosure: The authors declare no competing financial interests.

Correspondence: Lesley Bruce, Bristol Institute for Transfusion Sciences, NHS Blood and Transplant, North Bristol Park, Filton, Bristol, BS34 7QH, United Kingdom; e-mail: lesley.bruce@nhsbt.nhs.uk.

References

1. Stewart GW. Hemolytic disease due to membrane ion channel disorders. *Curr Opin Hematol.* 2004;11(4):244-250.
2. Bruce LJ, Robinson HC, Guizouarn H, et al. Monovalent cation leaks in human red cells caused by single amino-acid substitutions in the transport domain of the band 3 chloride-bicarbonate exchanger, AE1. *Nat Genet.* 2005;37(11): 1258-1263.
3. Bruce LJ, Guizouarn H, Burton NM, et al. The monovalent cation leak in overhydrated stomatocytic red blood cells results from amino acid substitutions in the Rh-associated glycoprotein. *Blood.* 2009;113(6):1350-1357.
4. Bruce LJ, Beckmann R, Ribeiro ML, et al. A band 3-based macrocomplex of integral and peripheral proteins in the RBC membrane. *Blood.* 2003; 101(10):4180-4188.
5. Fricke B, Jarvis HG, Reid CD, et al. Four new cases of stomatin-deficient hereditary stomatocytosis syndrome: association of the stomatin-deficient cryohydrocytosis variant with neurological dysfunction. *Br J Haematol.* 2004;125(6):796-803.
6. Lande WM, Thiemann PV, Mentzer WC Jr. Missing band 7 membrane protein in two patients with high Na, low K erythrocytes. *J Clin Invest.* 1982; 70(6):1273-1280.
7. Bruce LJ. Hereditary stomatocytosis and cation-leaky red cells–recent developments. *Blood Cells Mol Dis.* 2009;42(3):216-222.
8. Montel-Hagen A, Kinet S, Manel N, et al. Erythrocyte glut1 triggers dehydroascorbic acid uptake in mammals unable to synthesize vitamin C. *Cell.* 2008;132(6):1039-1048.
9. Weber YG, Storch A, Wuttke TV, et al. GLUT1 mutations are a cause of paroxysmal exertion-induced dyskinesias and induce hemolytic anemia by a cation leak. *J Clin Invest.* 2008;118(6): 2157-2168.
10. Brockmann K. The expanding phenotype of GLUT1-deficiency syndrome. *Brain Dev.* 2009; 31(7):545-552.
11. Klepper J, Scheffer H, Leiendecker B, et al. Seizure control and acceptance of the ketogenic diet in GLUT1 deficiency syndrome: a 2- to 5-year follow-up of 15 children enrolled prospectively. *Neuropediatrics.* 2005;36(5):302-308.
12. Leen WG, Klepper J, Verbeek MM, et al. Glucose transporter-1 deficiency syndrome: the expanding clinical and genetic spectrum of a treatable disorder. *Brain.* 2010;133(3):655-670.
13. Bruce LJ, Cope DL, Jones GK, et al. Familial renal tubular acidosis is associated with mutations in the RBC anion exchanger (band 3, AE1) gene. *J Clin Invest.* 1997;100(7):1693-1707.
14. Brant AM, McCoid S, Thomas HM, et al. Analysis of the glucose transporter content of islet cell lines: implications for glucose-stimulated insulin release. *Cell Signal.* 1992;4(6):641-50.
15. Leberbauer C, Boulmé F, Unfried G, Huber J, Beug H, Müllner EW. Different steroids co-regulate long-term expansion versus terminal differentiation in primary human erythroid progenitors. *Blood.* 2005;105(1):85-94.
16. Van den Akker E, Satchwell TJ, Pellegrin S, Daniels G, Toye A. The majority of the in vitro expansion potential resides in CD34(-) cells, outweighing the contribution of CD34(+) cells and significantly increasing the erythroblast yield from peripheral blood samples. *Haematologica.* 2010; 95(9):1594-1598.
17. Griffiths RE, Heesom KJ, Anstee DJ. Normal prion protein trafficking in cultured human erythroblasts. *Blood.* 2007;110(13):4518-4525.
18. Hiebl-Dirschmied CM, Adolf GR, Prohaska R. Isolation and partial characterization of the human erythrocyte band 7 integral membrane protein. *Biochim Biophys Acta.* 1991;1065(2):195-202.
19. Mueckler M, Caruso C, Baldwin SA, et al. Sequence and structure of a human glucose transporter. *Science.* 1985;229(4717):941-945.
20. Guizouarn H, Gabillat N, Motais R, Borgese F. Multiple function of a red blood cell anion exchanger tAE1: its role in cell volume regulation. *J Physiol.* 2001;535(2):497-506.
21. Martial S, Guizouarn H, Gabillat N, Pellissier B, Borgese F. Importance of several cysteine residues for the chloride conductance of trout anion exchanger 1 (tAE1). *J Cell Physiol.* 2007;213(1): 70-78.
22. Friesema EC, Ganguly S, Abdalla A, Manning Fox JE, Halestrap AP, Visser TJ. Identification of monocarboxylate transporter 8 as a specific thyroid hormone transporter. *J Biol Chem.* 2003;278(41):40128-40135.
23. Huang Y, Lemieux MJ, Song J, Auer M, Wang DN. Structure and mechanism of the glycerol-3-phosphate transporter from Escherichia coli. *Science.* 2003;301(5633):616-620.
24. Shen M-Y, Sali A. Statistical potential for assessment and prediction of protein structures. *Prot Sci.* 2006;15(11):2507-2524.
25. Davis IW, Murray LW, Richardson JS, Richardson DC. MOLPROBITY: structure validation and all-atom contact analysis for nucleic acids and their complexes. *Nucleic Acids Res.* 2004;32:W615-619.
26. Klepper J, Leiendecker B. GLUT1 deficiency syndrome–2007 update. *Dev Med Child Neurol.* 2007;49(9):707-716.
27. Pascual JM, Wang D, Yang R, Shi L, Yang H, De Vivo DC. Structural signatures and membrane helix 4 in GLUT1: inferences from human blood-brain glucose transport mutants. *J Biol Chem.* 2008;283(24):16732-16742.
28. Klepper J, Scheffer H, Elsaid MF, Kamsteeg EJ, Leferink M, Ben-Omran T. Autosomal recessive inheritance of GLUT1 deficiency syndrome. *Neuropediatrics.* 2009;40(5):207-210.
29. Fung EL, Ho YY, Hui J, et al. First report of GLUT1 deficiency syndrome in Chinese patients with novel and hot spot mutations in SLC2A1 gene. *Brain Dev.* 2011;33(2):170-173.
30. Suls A, Dedeken P, Goffin K, et al. Paroxysmal exercise-induced dyskinesia and epilepsy is due to mutations in SLC2A1, encoding the glucose transporter GLUT1. *Brain.* 2008;131(7):1831-1844.
31. Schneider SA, Paisan-Ruiz C, Garcia-Gorostiaga I, et al. GLUT1 gene mutations cause sporadic paroxysmal exercise-induced dyskinesias. *Mov Disord.* 2009; 24(11):1684-1688.
32. Salas-Burgos A, Iserovich P, Zuniga F, Vera JC, Fischbarg J. Predicting the three-dimensional structure of the human facilitative glucose transporter glut1 by a novel evolutionary homology strategy: insights on the molecular mechanism of substrate migration, and binding sites for glucose and inhibitory molecules. *Biophys J.* 2004;87(5): 2990-2999.
33. Hruz PW, Mueckler MM. Cysteine-scanning mutagenesis of transmembrane segment 7 of the GLUT1 glucose transporter. *J Biol Chem.* 1999; 274(51):36176-36180.
34. Mueckler M, Makepeace C. Transmembrane segment 12 of the Glut1 glucose transporter is an outer helix and is not directly involved in the transport mechanism. *J Biol Chem.* 2006; 281(48):36993-36998.
35. Carruthers A, DeZutter J, Ganguly A, Devaskar SU. Will the original glucose transporter isoform please stand up! *Am J Physiol Endocrinol Metab.* 2009;297(4):E836-E848.
36. Fricke B, Parsons SF, Knöpfle G, von Düring M, Stewart GW. Stomatin is mis-trafficked in the erythrocytes of overhydrated hereditary stomatocytosis, and is absent from normal primitive yolk sac-derived erythrocytes. *Br J Haematol.* 2005; 131(2):265-277.
37. Wang D, Pascual JM, Yang H, et al. A mouse model for Glut-1 haploinsufficiency. *Hum Mol Genet.* 2006;15(7):1169-1179.
38. Wang D, Pascual JM, Yang H, et al. Glut-1 deficiency syndrome: clinical, genetic, and therapeutic aspects. *Ann Neurol.* 2005;57(1):111-118.
39. Iolascon A, De Falco L, Borgese F, et al. A novel erythroid anion exchange variant (Gly796Arg) of hereditary stomatocytosis associated with dyserythropoiesis. *Haematologica.* 2009;94(8):1049-1059.
40. Guizouarn H, Borgese F, Gabillat N, et al. South-east Asian ovalocytosis is virtually indistinguishable from the cryohydrocytosis form of hereditary stomatocytosis. *Br J Haematol.* 2011;152(5):655-664.
41. Stewart AK, Vandorpe DH, Heneghan JF, et al. The GPA-dependent, spherostomatocytosis mutant AE1 E758K induces GPA-independent, endogenous cation transport in amphibian oocytes. *Am J Physiol.* 2010;298(2):C283-C297.
42. Merriman-Smith R, Donaldson P, Kistler J. Differential expression of facilitative glucose transporters GLUT1 and GLUT3 in the lens. Invest. *Ophthalmol Vis Sci.* 1999;40(13):3224-3230.
43. Fischbarg J, Diecke FP, Kuang K, et al. Transport of fluid by lens epithelium. *Am J Physiol.* 1999; 276(3 Pt 1):C548-C557.
44. Donaldson PJ, Chee KS, Lim JC, Webb KF. Regulation of lens volume: implications for lens transparency. *Exp Eye Res.* 2009;88(2):144-150.
45. Ruiz-Ederra J, Verkman AS. Accelerated cataract formation and reduced lens epithelial water permeability in aquaporin-1-deficient mice. Invest. *Ophthalmol Vis Sci.* 2006;47(9):3960-3967.
46. Salzer U, Mairhofer M, Prohaska R. Stomatin: A new paradigm of membrane organization emerges. *Dynamic Cell Biol.* 2007;1(1):20-33.
47. Zhang JZ, Hayashi H, Ebina Y, Prohaska R, Ismail-Beigi F. Association of stomatin (band 7.2b) with Glut1 glucose transporter. *Arch Biochem Biophys.* 1999;372(1):173-178.
48. Kumar A, Xiao YP, Laipis PJ, Fletcher BS, Frost SC. Glucose deprivation enhances targeting of GLUT1 to lipid rafts in 3T3-L1 adipocytes. *Am J Physiol.* 2004;286(4):E568-E576.
49. Komatsu T, Sato K, Otsuka Y, et al. Parallel reductions in stomatin and Na,K-ATPase through the exosomal pathway during reticulocyte maturation in dogs: stomatin as a genotypic and phenotypic marker of high K(+) and low K(+) red cells. *J Vet Med Sci.* 2010;72(7):893-901.
50. de Gassart A, Geminard C, Fevrier B, Raposo G, Vidal M. Lipid raft-associated protein sorting in exosomes. *Blood.* 2003;102(13):4336-4344.